2008 IEEE International Conference on
Robotics and Automation
Pasadena, CA, USA, May 19-23, 2008

Modeling and Fault Analysis of BLDC Motor Based Servo Actuators for Manipulators

Sewoong Kim, *Member*, *IEEE*

Abstract – This paper presents a modeling of brushless dc motor based servo actuator for manipulators, and described dynamic and fault analysis of the actuator using the model. A new model of brushless dc motors, which have delta windings, is proposed. Nonlinear model of the actuator, which has ball screw and spur gears, is presented, too. Nonlinear modeling of electromechanical actuation systems makes it possible to investigate the effects of faults such as open circuit of motor winding and jamming of gear screw. The simulation using the model examines the effects of nonlinear components on the system performance such as frequency response and dynamic stiffness which is more critical issue in some applications.

I. INTRODUCTION

The benefits of electromechanical actuation systems such as high reliability, facility of maintenance, and high power density due to high flux density of permanent magnets have been enhancing the use of electromechanical servo actuators in many applications where hydraulic systems have been used such as manipulators. Recent research on transmission-based actuators integrates multi-speed transmission, which has planetary gear set, with high speed BLDCM to make the power ratio of the actuator closer to hydraulic actuator [1], [2]. In high performance electromechanical actuator systems, permanent magnet synchronous motors (PMSMs) or brushless dc motors (BLDCMs) is usually used, and there are many discussions about the selection of the motors [3]. The use of BLDC motors in many area have been lead to a lot of studies in various aspects such as modeling and control in last decades [4]-[7]. In [7], Pillay and Krishnan developed a model of BLDC motors in natural abc frame instead of d-q rotating frame. In [8], Guinee and Lyden developed a model including nonlinear characteristics such as dead time of inverter and switching devices. In [10], M. A. Davis presented a nonlinear model of ball screw and gear of BLDCM based servo actuator.

The employment of the servo actuators in some areas, which require high performance and high reliability such as telerobots and aerospace applications, needs models describing not only nonlinear characteristics, but also fault characteristics. In the applications, human operators cannot access the platform to recover the system from faults since the task space is far away from human operators or the space is probably a hazardous environment. Therefore, fault detection and isolation (FDI) and fault tolerant control are strongly required in the systems [4],[9].

In the development of FDI and fault tolerant control strategies, nonlinear modeling of the system which describes fault operations of the systems is essential since fault injection experiments are difficult and costly. The FDI strategies usually analyze vibration, noise, and current in time or frequency domain to identify the signature of faults. There are not much useful models for vibration and noise analysis of actuation systems. But there are several researches to describe motor currents in fault conditions. In [9], Wallace *et al* developed a model including switching devices, and it can simulate motor winding failure. However, it cannot simulate the failure of switching devices, which are like to occur in many systems. In many researches, it is assumed that the motor has wye winding instead of delta winding which is generally used below medium power range because the winding process is simpler than that of wye. In normal operation, wye winding models equivalently represent delta winding BLDCM since the line currents of both windings are similar. However, in unbalanced or fault operation conditions, the wye winding model cannot equivalently represent delta winding motor since the wye model cannot simulate phase currents of delta winding which generate motor torque by interacting with magnet flux.

This paper presents a nonlinear modeling of a BLDC motor based servo actuator for fault analysis. The model includes a new analysis for delta winding BLDC motors. It also modeled a switching device of inverter, a ball screw, and other nonlinearities such as dead time, backlash, etc. In this paper, instead of transmission based servo actuator based on planetary gears [1], ball screw and spur gear power train is considered for generalization. The model is used to simulate not only the dynamic characteristics, but also fault operation. The simulation results of the fault operation and dynamic analysis of the system are discussed.

II. Modeling of Actuation systems

2.1 Modeling of Delta Winding BLDC Motor

Fig. 1 is a schematic of three phase delta winding BLDC motor and inverter. Line-to-line voltage equations of the system in natural abc frame are (1). If the upper switch in a leg is turned on, the pole voltage is $V_d/2$. If the lower switch in a leg is turned off, the pole voltage is $-V_d/2$. If

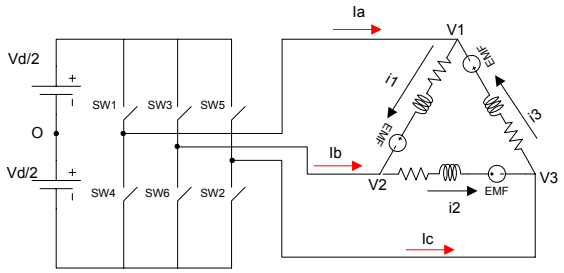

Fig. 1 Schematic of delta winding BLDC motor and inverter.

both of two switches are turned off, the pole voltage depends on the other two pole voltages.

$$\begin{aligned} V_{1o} - V_{2o} &= R_1 i_1 + L_1 \frac{di_1}{dt} + E_1 \\ V_{2o} - V_{3o} &= R_2 i_2 + L_2 \frac{di_2}{dt} + E_2 \\ V_{3o} - V_{1o} &= R_3 i_3 + L_3 \frac{di_3}{dt} + E_3 \end{aligned} \quad (1)$$

where V_{1o}, V_{2o},V_{3o} are pole voltages, which are terminal voltages relative to the dc mid-point O..

For examples, if SW_1 is turned on and SW_4 is turned off, V_{1o} is = V_d/2.If SW_1 is turned off and SW_4 is turned on, V_{1o} is -V_d/2. When two switches SW_1 and S_4 are turned off, and SW_3 of phase B and SW_2 of phase C are turned on (Fig. 2 (a)), the line-to-line voltage is

$$V_{3o} - V_{2o} = (R_1 + R_3) i_2 + (L_1 + L_2) \frac{di_3}{dt} + E_1 + E_3 \quad (2)$$

In balanced condition, the resistances and inductances are same, and therefore

$$V_{3o} - V_{2o} = 2Ri_1 + 2L\frac{di_1}{dt} + E_1 + E_3 = 2Ri_1 + 2L\frac{di_1}{dt} - E_2 \quad (3)$$

When motor conduction mode is Fig. 2 (a), $V_{2o} = V_d / 2$, $V_{3o} = -V_d / 2$, and $i_1 = i_3$, so that

$$\begin{aligned} \frac{V_d}{2} + \frac{E_2}{2} &= Ri_1 + L\frac{di_1}{dt} \\ \frac{V_d}{2} + \frac{E_2}{2} &= Ri_3 + L\frac{di_3}{dt} \end{aligned} \quad (4)$$

Adding E_1 and E_3 to both sides of (4), we obtain

$$\begin{aligned} \frac{V_d}{2} + \frac{E_2}{2} + E_1 &= Ri_1 + L\frac{di_1}{dt} + E_1 \\ \frac{V_d}{2} + \frac{E_2}{2} + E_3 &= Ri_3 + L\frac{di_3}{dt} + E_3 \end{aligned} \quad (5)$$

Substituting (1) into (5), and solving the equation, pole voltage is given by

$$V_{1o} = \frac{E_1 - E_3}{2} \quad (6)$$

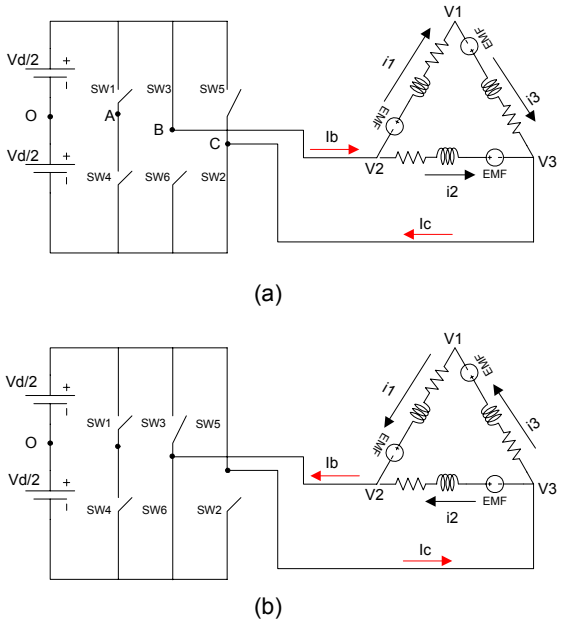

Fig. 2 Conduction and commutation mode of the BLDC motor and inverter.

The other two pole voltages are derived in a similar manner, and when two switches of a leg are turned off simultaneously, the pole voltage in balanced condition is represented in general form as

$$V_{ko} = \frac{E_k - E_{k-1}}{2}, k = 1,2,3 \quad (7)$$

Healthy operation of BLDC mtors in balanced condition is modeled by (1) and (7). Although the motor parameters are not exactly same, the unbalance of the parameters is usually small and the effects of the unbalanced parameters are negligible. However, if unbalance is increased, the effects of the unbalance are not negligible and the pole voltage of (7) is not valid any more. If BLDC motor having large unbalanced parameters is in the conduction mode of Fig. 2(a), phase current $i_2 = i_3$ and we obtained phase current i_3 from (2) as

$$I_3 = \frac{V_{3o} - V_{2o} - E_1 - E_3}{(L_1 + L_3)S + (R_1 + R_3)} + E_1 + E_3 \quad (8)$$

where S is differential operator. Solving (1) and (8), the pole voltage is given

$$V_{1o} = V_{3o} - [V_{3o} - V_{2o} - (E_1 + E_3)] \frac{L_3 S + R_3}{(L_1 + L_3)S + (R_1 + R_3)} \quad (9)$$

The other two pole voltages in unbalanced condition are set up in the same way. When two switches in a leg are turned off, the general representation of the pole voltage is

$$V_{ko} = V_{k-1} - [V_{k-1o} - V_{k+1o} - (E_k + E_{k-1})] \frac{L_{k-1}S + R_{k-1}}{(L_k + L_{k-1})S + (R_k + R_{k-1})} \quad (10)$$

$k = 1,2,3$

The faults occurred in BLDCMs can be represented by the unbalanced BLDCM models since open faults in motor winding can be represented with very high impedance of the phase, and short faults in motor winding can be represented with short circuit of the phase. Thus, the unbalanced model is used for the analysis of the faults

2.2 Modeling of Ball Screw Power Train

Fig. 3 shows a configuration of brushless dc motor based electromechanical servo actuator having a ball screw. It consists of a spur gear reduction, a ball screw, a moment arm, and a joint axis. The motor speed is reduced by the spur gear, and the ball screw reduces and converts the output of the spur gear to reciprocation motion. The moment arm converts the reciprocation motion into rotation motion at joint axis. The actuator has a tachometer at the end of BLDCM and a potentiometer at joint axis.

The generating torque of the BLDCM are transmitted through the spur gear, and the transmitted torque is expressed by

$$T_m = J_m \frac{d\omega_m}{dt} + B_m \omega_m + T_f + T_s$$
$$T_s = K_s(\theta_m - \theta_s / N_s) + C_s(\omega_m - \omega_s / N_s) \quad (11)$$

where T_m is the generating torque, J_m is the moment of inertia, B_m is the viscous damping, ω_m is the angular velocity, θ_m is the angle, and T_f is the friction torque of the motor. T_s is the transmitted torque through the spur gear, θ_s is the angle, ω_s is the velocity, K_s is the elasticity, C_s is the inner damping coefficient, and N_s is the turn ratio of the spur gear.

The orientation (θ_1) of the ball screw with respect to the hinge point changes as the joint rotates, and the effective linear increment of the ball screw is a function of the orientation of the ball screw, the increment of the rod length (L, L'), the angular position of the joint (θ_j), and the length of the moment arm (R) as shown in Fig. 4.

From the relationship, the transmitted force through the ball screw and spur gear is expressed as

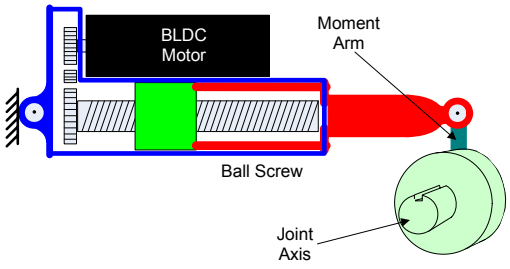

Fig. 3 BLDCM based servo actuator with ball screw.

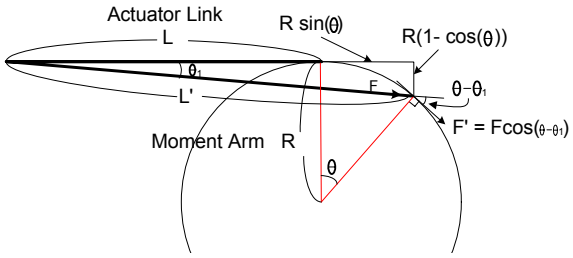

Fig. 4 Geometrical relationship of the transmitted force and joint torque.

$$T_s = J_{sp} \frac{d\omega_s}{dt} + B_{sp}\omega_s + T_f + P_L F_b$$
$$F_b = K_{sb}(P_L\theta_s - (L' - L)) \quad (12)$$
$$= K(P_L\theta_s - (\sqrt{(L + R\sin\theta_j)^2 + (R(1-\cos(\theta_j)^2} - L))$$

where F_b is the transmitted force through the ball screw, J_{sp} is the moment of inertia of the ball screw, B_{sp} is the viscous damping of the ball screw, K_{sb} is the elasticity of the ball screw, P_L is the pitch of the ball screw, L is the length of the ball screw when the joint angle is zero, R is the length of the moment arm.

The generating torque at the joint is derived using the transmitted force (F') and the moment arm (R). The geometrical relationship is shown in Fig. (4), and the torque is computed as

$$T_j = F_b' R = F_b R\cos(\theta j - \tan^{-1}(\frac{R(1-\cos\theta j)}{L + R\sin\theta j})$$
$$= J_j \frac{d\omega_j}{dt} + B_j\omega_j + T_L \quad (13)$$

where T_j is the joint torque, θ_j is the angular position of the joint, J_j is the moment of inertia of the joint, B_j is the viscous damping of the joint, ω_j is the angular velocity of the joint, T_L is the load torque of the joint

2.3 Modeling of Switching Device

Switching devices used in the inverter for BLDCM servo actuator are usually IGBT or MOSFET, and they have diodes called freewheeling diode, which are connected in anti-parallel, and provides freewheeling path for the motor line currents. In this paper, the switching device and the

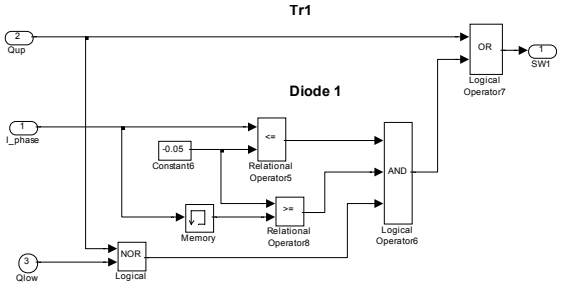

Fig. 5 Ideal model of switching device and diode.

freewheeling diodes are assumed as an ideal switch. Fig. 5 shows the model of the ideal switch and freewheeling diode used in this study.

III. System Configuration and Experiments

The BLDCM based servo actuator system consists of two main parts: 1) manipulator joint configuration with passive spring load, and 2) digital controller. As shown in Fig. 6, the joint configuration includes 1.5kw BLDC motor, ball screw/spur gear drive, and 70lbf-in/deg passive spring load. The digital controller has TMS320c32 DSP for outer loop position control, and FPGA is used for PWM current control. The test & data acquisition system based on Pentium 4 PC with Windows 2000 send reference command to the controller, and acquire and save sensor data and for offline data analysis.

Fig. 7 shows the experiment result of the servo actuator, and Fig. 8 shows the simulation result using the model. The test and simulation was conducted without load. Fig. 7 (a) and Fig. 8(a) are the angular position of the actuator, and Fig. 7(b) and Fig. 8(b) are the speed of the BLDCM. It shows that the BLDCM speed builds up in less than 20ms, and the speed is almost constant until the actuator position reached the set position. The motor starts to rotate in reverse direction after it reached the set position to compensate the

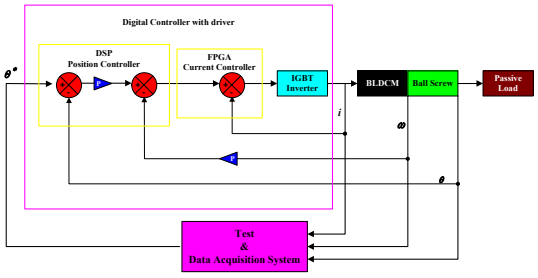

Fig. 6 Control block diagram of the system.

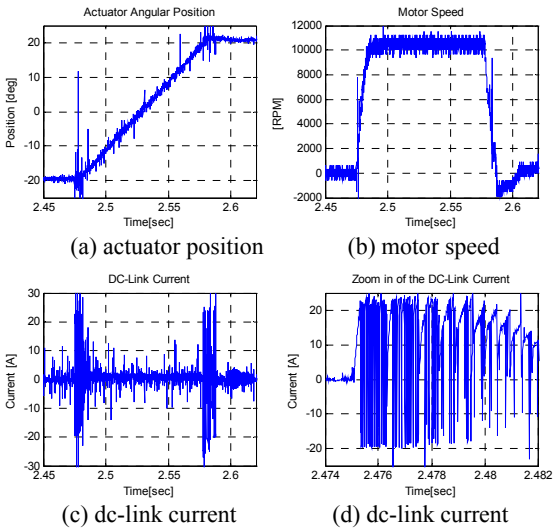

(a) actuator position (b) motor speed

(c) dc-link current (d) dc-link current

Fig. 7 Experiment results of BLDCM based servo actuator.

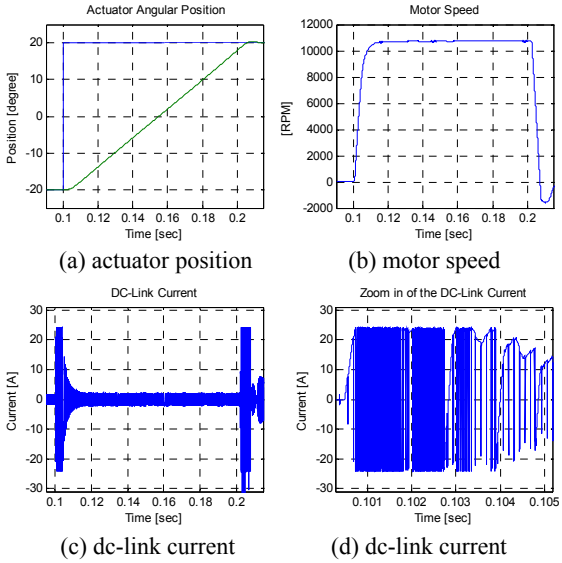

(a) actuator position (b) motor speed

(c) dc-link current (d) dc-link current

Fig. 8 Simulation result of the BLDCM servo actuator.

overshoot. Fig. 7(c) and Fig. 8(c) are the dc-link current. It shows that the magnitude of the dc-link current is high when the actuator starts and stops. When it started, the effective dc-link current flowed into the motor to supply a power for starting torque. When the switching devices are turned off, the effective dc-link current flows back into to the dc-link capacitor from the BLDCM. Fig. 7 (d) and Fig. 8(d) are enlarged picture of the dc-link current when the motor started. Fig 9 is the frequency response test results. The comparisons of the experimental tests and simulation tests

(a) Experiment result

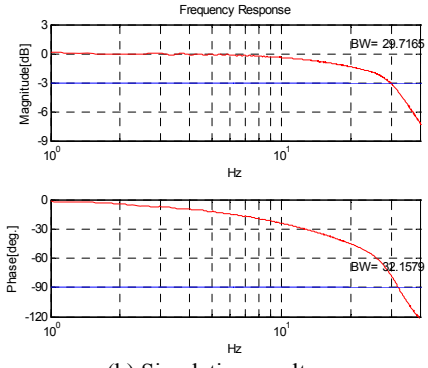

(b) Simulation result

Fig. 9 Frequency response test results.

show that not only the model simulates the actuator parameters such as the position, speed, and frequency response, but also the internal parameters such as currents. In this research, the current simulation ability of model is important since the current information will be used to develop FDI algorithms in near future.

IV Simulation Results for Fault Analysis

4.1 Normal operation analysis

Fig. 10 (a), (b) are the phase and line currents of the delta winding BLDCM when it operates with load. It shows that the line current of delta winding is similar to that of wye winding motor. Thus, delta winding BLDC motor can be represented by equivalent wye BLDCM. Fig. 10 (c) is the dc-link current when the commutation strategy is pseudo 4 quadrant method. In the method, the switches in the conduction path are turned on and off simultaneous. The dc-link current flows into the BLDCM when the switches are turned on simultaneous. The dc-link current flows back into the dc-link capacitor through the freewheeling diodes when the switches are turned off simultaneous. The simulation results show that the developed model simulates the currents: motor phase current, line current, and dc-link current. Since the model can simulate the phase current, it can present abnormal operation caused by unbalanced phase current.

4.2 Open fault of motor armature winding

Fig. 11 shows the position of the actuator, the dc-link voltage, the motor phase currents, and the motor line currents when an open fault of the motor winding occurs in phase 1. In this simulation, it is assumed that a robot arm, which has large moment of inertia, is installed in the joint with spring load having 70lbf-in /deg elasticity. It shows that when the open fault occurs, the phase current of the fault phase does not flow. However, the other two phase currents (phase 2, phase 3) are increased to compensate the reduction of torque. Unlike wye winding BLDCM, delta winding BLDCM can operate with the open fault and this is

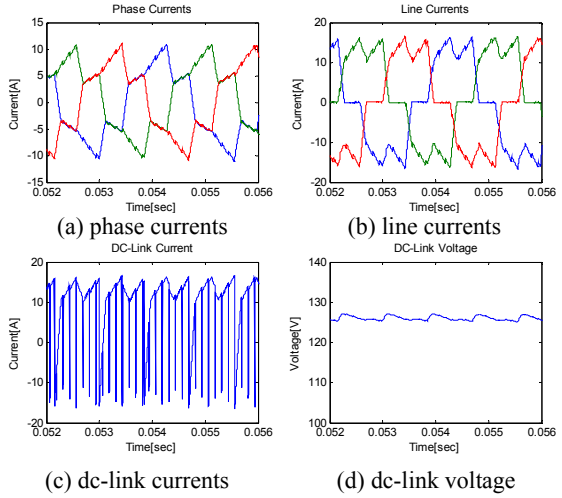

(a) phase currents (b) line currents

(c) dc-link currents (d) dc-link voltage

Fig. 10 Simulation results of BLDCM based servo actuator.

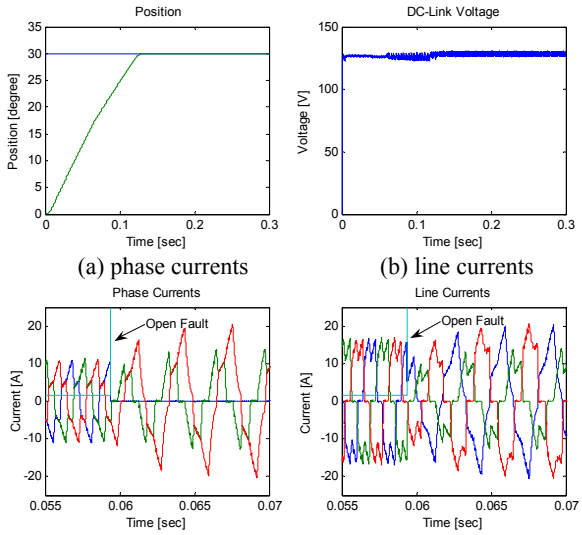

(a) phase currents (b) line currents

(c) phase currents (d) line currents

Fig. 11 Open fault of motor winding.

an inherent fault tolerant characteristic of BLDCM. Although the phase current cannot flow in the fault phase, line currents flow in all three lines. Thus, if the line currents or dc-link current are not measured properly, the open fault cannot be detected and the system will be damaged by overheat

4.3 Open fault of switching device

Fig. 12 shows the effects of open faults in the switching devices. Fig. 12 (a) shows the currents and position when the upper switching device and freewheeling diode are open circuited. Open faults of the devices make the effective line current do not flow in the fault line. The generating torque is reduced and the actuator cannot operate with the load. If only the switching device is open circuited, negative line current can flow through the freewheeling diode. The generating torque is higher than that of the open faults in the two devices, and the actuator can operates with the load. Although, the actuator can operate with the open fault of switching devices, the fault must be detected and the current must be limited since the phase and line currents are increased after the fault.

4.4 Failure in the thread of ball screw

The actuator can be jammed in operation by failures in the thread of the ball screw, and insufficient lubricant is one of the origins, which cause the failure. After the fault, if the normal control strategies are applied without removal of the fault, the system will be damaged. If a strategy applied to free the jammed screw is improper, the operation can lead to complete failure [11]. In this paper, it is assumed that the fault can be modeled by the sudden increment of the frictions of the ball screw. Fig. 13 is the simulation results. It shows that the position of the actuator is frozen, and the maximum current flows through the line. Thus, if the fault is not detected and the current is not limited by the controller, the system will be damage by the overload operation.

V. Conclusion & Future Works

The modeling of brushless dc motor based servo actuator and the fault analysis of the system using the model are discussed. The proposed new model of BLDCM having delta winding shows not only the line currents, but also the phase currents, which are not usually observable. It shows that the analogousness between the line currents of the wye and delta winding BLDCM. The BLDCM model is useful to estimate and observe the phase current from the line currents, and to decide motor operating condition. The nonlinear model of the servo actuator including the inverter and ball screw shows how the system parameters will change after the faults such as the open circuit of motor winding and the jamming of gear train. The nonlinear model will save time and expense in the development of a fault detection and isolation (FDI) and fault tolerant control algorithms. In the continuing research, author will explore the FDI and graceful degradation algorithms for the faults. With the algorithms, the system can continue to operate with reduced power ability rather than sudden complete system shut down. In many applications, the required power in most operating time is less than the rated power and system may not experience any performance degradation after the faults.

VI. Reference

[1] W. R. Hamel, Sewoong Kim, R. Zhou, and A. Lumsdaine, "Dynamic Modeling and Analysis of a Transmission-based Robot Servoactuator," Proceedings of the 2003 IEEE International Conference on Robotics and Automation, pp.208~213, 2003.

[2] W. R. Hamel, Sewoong Kim, R. Zhou, and A. Lumsdaine, "Design and testing of a prototype transmission-based robot servoactuator," Proceedings of the 2004 IEEE International Conference on Robotics and Automation, pp.3628~3633, 2004.

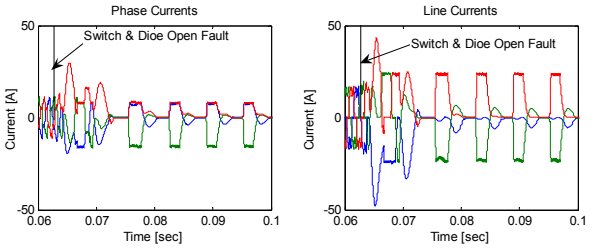

(a) open fault in switching device & diode

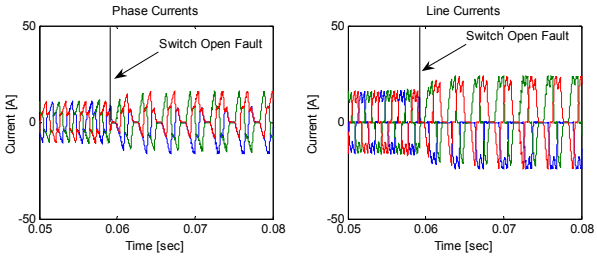

(b) open fault in switching device only

Fig. 12 Open fault of switching device.

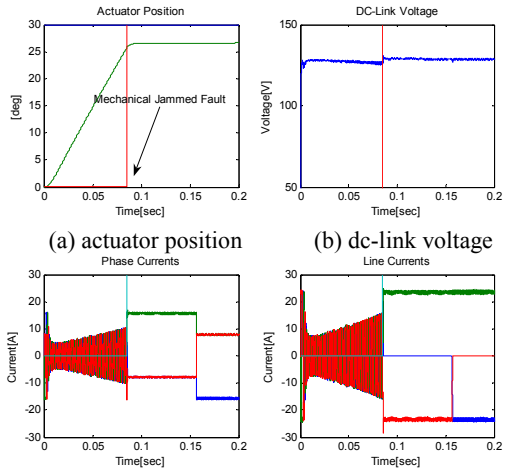

(a) actuator position (b) dc-link voltage

(c) phase currents (d) line currents

Fig. 13 Broken fault of the ball screw rod.

[3] G. Liu, W.G. Dunford, "Comparison of Sinusoidal Excitation and Trapezoidal Excitation of a Brushless Permanent Magnet Motor," Fourth International Conference on Power Electronics and Variable-Speed Drives, pp.446~450, 1990.

[4] Sewoong Kim, William R. Hamel, "Design of Supervisory Control Scheme for Fault Tolerant Control of Telerobotic System in operational Space," Proceedings of the 2003 IEEE/RSJ International Conference on Intelligent robots and Systems, pp. 2803~2807, 2003.

[5] S. K. Safi, P. P. Acarnley, and A. G.Jack, "Analysis and simulation of the high-speed torque performance of brushless DC motor drives," IEE Proc. Electr. Power Appl., Vol. 142, No.3, pp. 191~200, May 1995.

[6] R. C. Becerra, M. Ehsani, and T. Jahns, "Four Quadrant Brushless ECM Drive with Integrated Current Regulation," Industrial Application Society Annual Meeting, vol.1, pp. 819~828, 1989.

[7] Pragasen Pillay, Ramu Krishnan,"Modeling , Simulation, and Analysis of Permanent-Magnet Motor Drives, Part II: The Brushless DC Motor Drive," IEEE Transactions on Industry Applications, Vol. 25, No.2, pp. 274~279, March/April, 1989

[8] R. A. Guinee, C. Lyden, "Accurate Modelling and Simulation of a DC Brushless Motor Drive System for High Performance Industrial Applications," Proceedings of the 1999 IEEE International Symposium on Circuits and System, vol.5, pp. V-106~V-109, 1999.

[9] Alan K. Wallace, René Spee, "The Simulation of Brushless DC Drive Failures," Power electronics Specialists Conference PESC '88, Vol.1, pp.199-206, 1988.

[10] M. A. Davis,"High Performance Electromechanical Servoactuation Using Brushless DC Motors," Technical Bulletin 150, Moog Inc, East Aurora, New York, 1984.

[11] Mattias Nordin, Per-Olof Gutman,"Controlling mechanical systems with backlash – a survey," Automatica, vol. 38, pp.1633~1649, 2002.